STUDY ON IDENTIFICATION OF CHARACTERISTICS OF THORAX OF THOR-M50 (METRIC)

HyunJae Park
AHyun Cho
Taewung Kim
Korea Polytechnic University
Korea

MinGi Cho
TaeHee Lee
SooYul Lee
Wook Jin
Hyundai Motor Group
Korea

Moonkyu Lee
Sogang University
Korea

Paper Number 19-0337

ABSTRACT

The current study aimed to characterize the structural responses of the thorax during compressive loading conditions to aid interpret the behavior of the thorax during more complex loading conditions or validate computational THOR dummy models. A series of quasi-static compression tests were performed for individual ribs and the thorax complex using two types of indenters. For a rib compression test, an indenter with a 10 mm diameter was used to load the end of a rib. This indenter was installed on a linear guide array to minimize the application of shear forces to the dummy. The influence of the thoracic bib was investigated by performing this test with and without the bib. The displacements of the other ribs were measured using a three-dimensional motion tracking system. Another 52 mm by 104 mm indenter was used to apply more belt-like loading to the loading site. From these two series of tests, stiffness was calculated using the applied force at 25.4 mm of compression. In addition, compliances of the four thoracic IR-TRACC sites (rib 3 and 6) were calculated using the applied force at 25.4 mm of compression and deflection of the IR-TRACCs. During the rib compression test without the bib, the 7th rib exhibited the highest stiffness (2.3 N/mm) while the stiffness of other ribs ranged from 0.8 to 1.5 N/mm. During the rib compression test with bib, the 1st rib region demonstrated the highest stiffness (17 N/mm), while the stiffness of other regions ranged from 6.8 to 11.3 N/mm. The bib increased the rib stiffness substantially, and its effect was the highest for the 1st rib region. The compliance results indicated that the IR-TRACC deflection is mainly influenced by the forces applied to the ribs that the IR-TRACC was installed and their adjacent ribs, e.g. rib 2 and 4 for the upper thoracic IR-TRACC, on the same side. The thoracic responses of the THOR-M50 obtained from the current study can be utilized in model validation and interpretation of the response of the thorax during more complicated loading conditions such as crash test.

INTRODUCTION

THOR (Test device for Human Occupant Restraint) dummy is expected to be introduced in the new car assessment program in the US and Europe to assess injury risk of occupants during frontal crash scenarios (Shaw et al., 2004, Yaguchi et al., 2008, Lebarbé et al., 2012, Lemmen et al., 2012). THOR dummy differs from the Hybrid III frontal crash dummy in terms of mechanical structure (Shaw et al., 2005). In addition, the number of measurement locations of the chest deflection has been increased from one to four compared to the Hybrid III dummy. Due to these

differences, THOR and Hybrid III dummies demonstrated different chest deflection during 48 km/h frontal sled tests (Shaw et al., 2000 biofidelity evaluation of the THOR advanced frontal crash test dummy, IRCOBI). During the test, the THOR dummy showed more PMHS-like anterior chest wall movement than did the Hybrid III. Also, THOR showed more PMHS-like interaction with the restraint in terms of the shoulder and lap belt loads. Sunnevång et al. (2014) evaluated the sensitivity of the thoracic regions of THOR and Hybrid III dummies under frontal sled conditions. Chest deflection responses of THOR dummy was more sensitive to the change of the configurations of the restraint systems, which included belt load limiter and driver airbag, than was the Hybrid III. Although the frontal sled test is useful to investigate the sensitivity of the THOR responses to the changes of the restraint systems, it is difficult to deduce mechanisms for the sensitivity due to the dynamic nature of the crash test conditions and complex loading conditions that the dummy experience.

As a first step to understand the interaction between the thoracic region of the THOR dummy and the safety belt system, the current study aimed to characterize the structural responses of the thorax during a series of compression tests under quasi-static loading conditions. The thoracic region of the THOR dummy was mounted to a test fixture through its upper spine structure and loaded using a 10 mm diameter indenter with and without the thoracic bib. Another series of the thorax indentation test was performed by mimicking the test condition from Shaw et al (2005).

METHOD

Dummy Positioning

The THOR dummy without its jacket was mounted to a uniaxial material testing machine through its upper spine structure (See Figure 1). The rib 3, 5, and 7 were used to fix the upper spine to the test fixture. The dummy was positioned so that the levels of the back of the rib 5 and 7 are the same with each other. Its pelvic region was simply supported using a horizontal bar to maintain its seating posture. After the positioning, the inclination of the thoracic surface at the center at the middle of the upper IR-TRACC was 2 degrees, which means the toward the head is downhill. Please note that the rib support was used only for the thorax compression test.

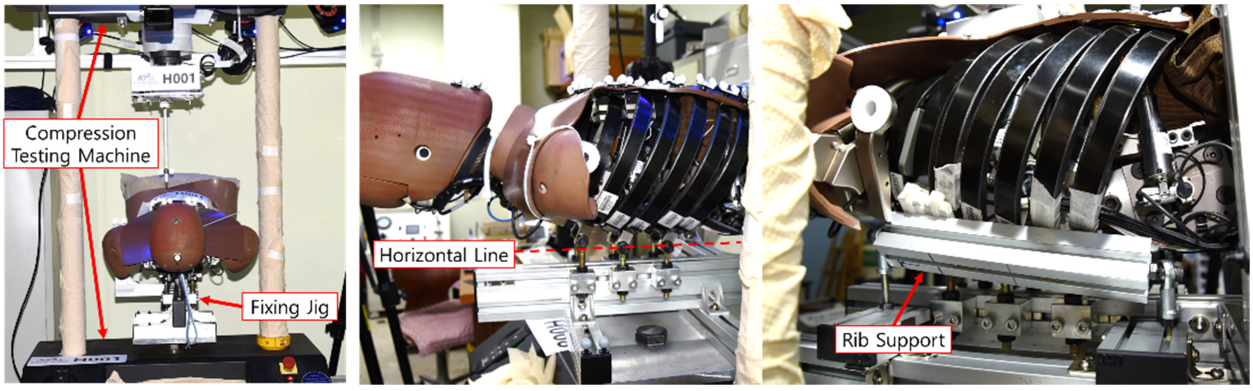

Figure 1 Dummy Positioning

Test Conditions

Rib compression test Rib compression test was performed using 10 mm diameter and 250 mm long indenter with and without the thoracic bib (See Figure 2). The end hole of each rib on the seven levels was loaded by the indenter. The end of the indenter was fabricated so that its surface becomes concave with 9 mm of the radius of curvature. The bolt at the end of the rib was replaced to the cup square neck bolt of which the radius of curvature of the head was 9 mm. The end of the indenter and the head of the bolt behaved like a ball-socket joint during the testing. The mating surface of the indenter and the head of the bolt was lubricated prior to each test. The indenter

holder consisted of two linear guides, which were perpendicular to each other so that the loading site can be translated in shear directions during the test. The loading rate was 1.7 mm/s, and the maximum compression amount ranged from 35 mm to 45 mm depending on the loading site. Each test was performed at least three times to calculate average values.

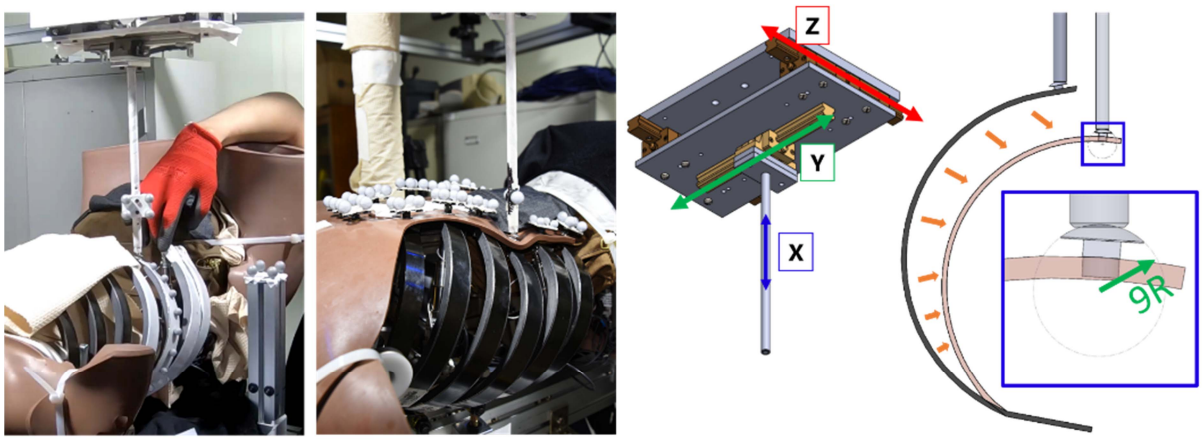

Figure 2 Indentor of rib compression test and indenter holder

Thorax compression test Thorax compression test was performed using an indenter, which the area of the contacting surface was 52 mm by 104 mm (Shaw et al., 2005, Cavanaugh et al., 1988). Following the procedure from Shaw et al. (2005), the indenter was installed to the test fixture through a ball-socket joint, which allowed around 27 degrees of rotation. The distance from the center of the rotation of the joint and the loading surface was 60 mm (See Figure 3). Three locations along the centerline of the thorax and three off centered locations were loaded (Shaw et al., 2005). Six locations, which were right-up, right-mid, right-low, stern-up, stern-mid, stern-low, was loaded with the bib installed. The indenter was rotated 30 degrees from the vertical line for the right-up and right-low tests. Twenty-five newtons of the preload was applied to ensure proper contact between the thorax and the indenter. The test was performed three times for each loading site with 1.7 mm/s of the loading rate and the 40 to 50 mm of the maximum compression amounts.

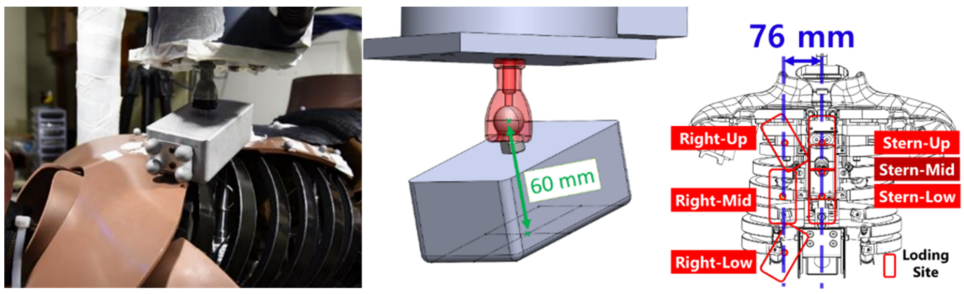

Figure 3 Indenter and indenter holder for the thorax compression test

Data Collection

The compressive force was measured using a uniaxial loadcell. The three-dimensional deformation of the thoracic and abdominal regions was measured using the built-in IR-TRACC sensors. For the rib compression test, the deformation of the other ribs without IR-TRACC installed was measured using a three-dimensional motion capture system (VICON MX^{TM}). The upper thoracic IR-TRACC (UT) and lower thoracic IR-TRACC (LT) were at the rib 3 and rib 6, respectively. For the following analysis, deflection along the direction of the compression, which was X-axis in Figure 1, was considered. The deformation of the unloaded site was calculated using the motion tracking data along the X-axis (See Figure 2). There were differences between the location of the marker and the center of the holes at the end of each rib. The displacement of the center of the hole was estimated based on the four markers attached to the end of the rib through a rigid body transformation scheme.

The stiffness was calculated using the force measured from the uniaxial loadcell at 25.4 mm of the displacement of the test device. For the rib compression test with bib and the thorax compression test, compliance, which is the deflection over the force, was calculated for the rib 3 and rib 6 where the IR-TRACC was installed. As a result, four compliance values were obtained for each test. For example, when right-side rib 2 was compressed 25.4 mm along the X-axis, the force was 0.19 kN and the right upper IR-TRACC indicated 11 mm of compression (See Figure 4). It resulted in 57 mm/kN of the compliance for the loaded-side upper thorax. During the rib compression test with bib, the coupling effect from the bib was evaluated using the displacement along the X-axis of the unloaded sites normalized to that of the loaded site, which was 25.4 mm.

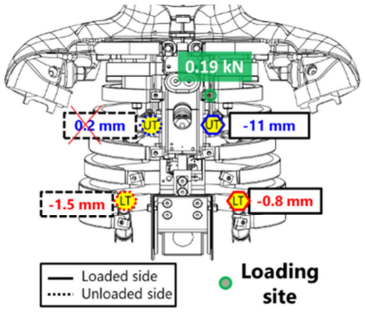

Compliance X-only	Loaded side [mm/kN]	Unloaded side [mm/kN]
UT	**57**	**0**
LT	**7**	**4**

Figure 4 Calculation of the compliance

RESULTS

Stiffness

For the rib compression test, the stiffness of the individual ribs (no bib condition) ranged from 0.8 to 2.3 N/mm (See Figure 5). When the bib was installed, the stiffness of each loading site increased from 5 to 14 times compared to the no bib condition. For the thorax compression test, the stiffness of the central area was higher than that of the corresponding off centered area.

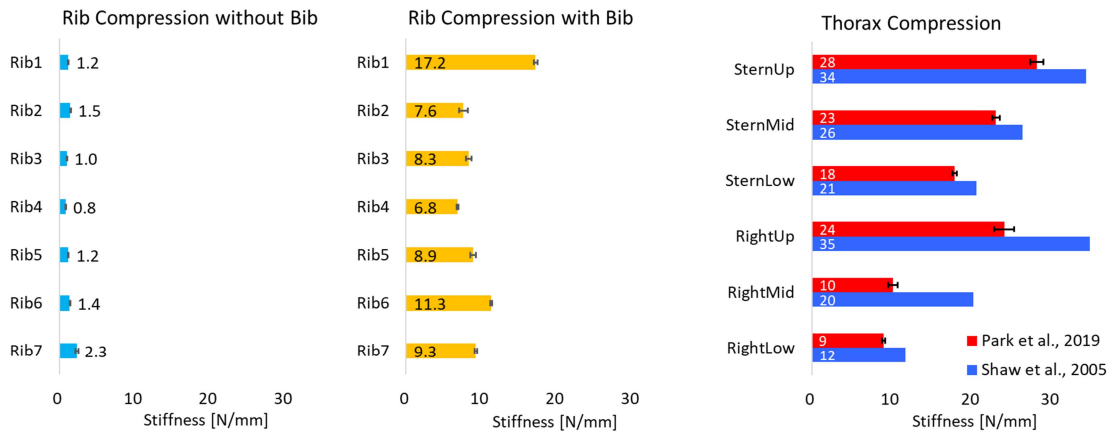

Figure 5 Summary of stiffness at 25.4 mm compression of the loading sites

Deflections of Coupled Ribs

The degrees of coupling between the loaded site and unloaded site varied depending on the loading site (See Figure 6). The coupling effect between upper and lower rib was higher than that of the loaded-side and unloaded-side except for the rib 1.

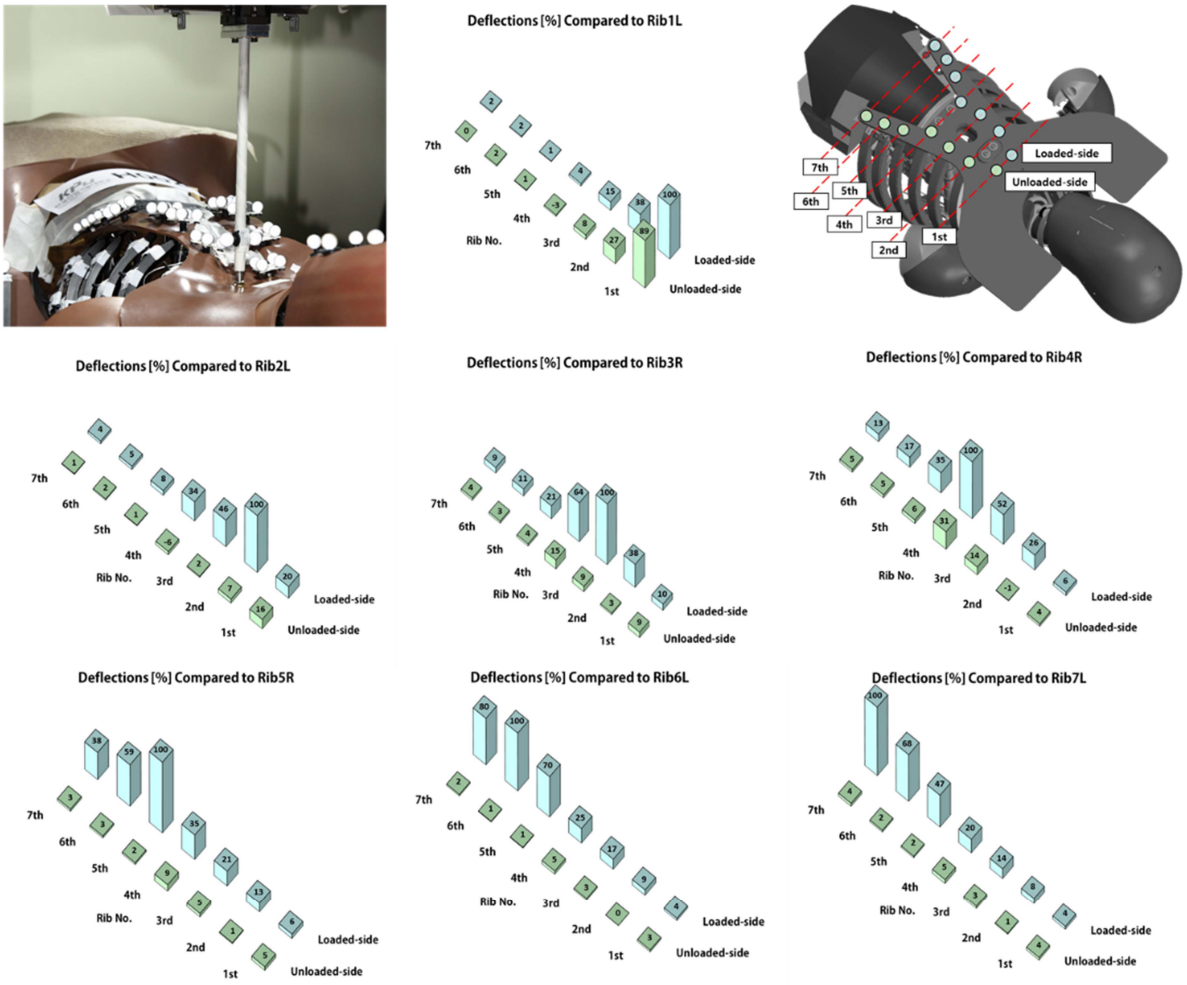

Figure 6 Summary of normalized compression amount during the rib compression tests with bib

Compliance Data

Rib compression test For the loaded side, the compliances of the upper and lower thorax showed maximum value at the rib 3 and rib 6, respectively. The compliance values for the unloaded side was less than 20 mm/kN for all the loading sites.

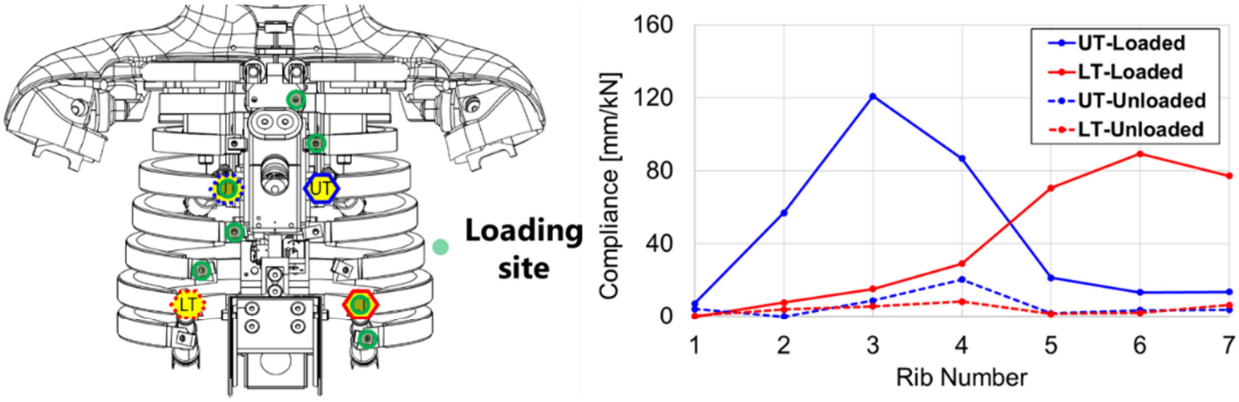

Figure 7 Compliance of four IR-TRACC sensors for each loaded rib

Thorax compression test The thorax compliance map was created by mirroring the right-side data to the left side (See Figure 8).

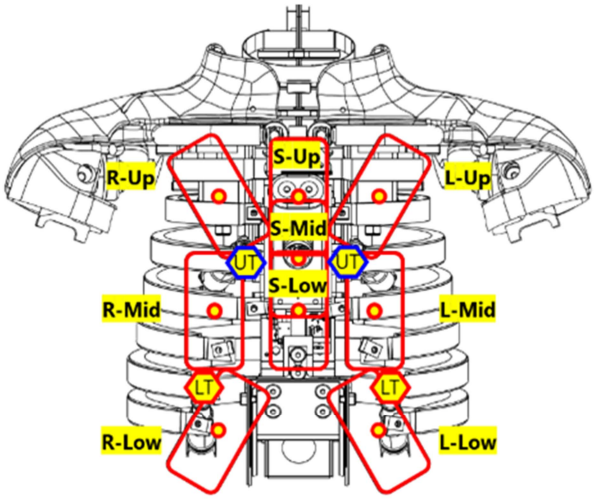

R-Up	Right	Left
UT	33	0
LT	2	1

S-Up	Right	Left
UT	20	20
LT	1	1

L-Up	Right	Left
UT	0	33
LT	1	2

S-Mid	Right	Left
UT	37	37
LT	2	2

R-Mid	Right	Left
UT	74	8
LT	52	0

S-Low	Right	Left
UT	41	41
LT	1	1

L-Mid	Right	Left
UT	8	74
LT	0	52

C=dx/F [mm/kN]
C: compliance

R-Low	Right	Left
UT	2	-4
LT	68	2

L-Low	Right	Left
UT	-4	2
LT	2	68

Figure 8 Compliance of four IR-TRACC sensors for each loaded site

DISCUSSION

A series of the thoracic compression test was performed using the THOR M50 (Metric) dummy under quasi-static loading conditions to characterize its behavior under compressive loading condition. Since the maximum deflection amount of any IR-TRACCs is used for the injury risk assessment, the emphasis was given to the deflection of the IR-TRACCs. Because of the simplified loading and boundary conditions, the test results will be useful for the THOR dummy computational model validation. During the rib compression tests, a pair of linear guides were used no to impose shear force to the rib. While the linear guide was well lubricated and it required less than 10 N to slide

in each direction under the unloaded condition, the shear force applied from the indenter to the rib during the test is unknown. During the thorax compression test, there was 60 mm of offset between the loading surface and the center of the ball-socket. This offset and the rotation of the indenter for the thorax compression test resulted in the shift of the loading sites as the joint rotated. In addition, the joint allowed the rigid body rotation of the indenter so that part of the displacement might have not resulted in the compression of the thorax. For this reason, the compliance of the thoracic IR-TRACC was calculated, which measured internal deformation. While the shear forces from the indenters to the loading sites are unknown from the current tests, the rib compression test results are less limited thanks to the linear guide for the model validation purpose.

During the rib compression test, the thoracic bib increased the stiffness of the loading site by a factor of 5 to 14. The bib created coupling between the loaded rib and unloaded ribs. Although we consider the contribution of the unloaded ribs by multiplying the stiffnesses of the unloaded ribs and compression amount due to the coupling, these amount of increase in the stiffness is not explained entirely. From the separate investigation of the three-dimensional motion tracking data, it was found that the shear displacements of the ribs during compression was decreased. It was estimated that the effects of the coupled deflection along the X-axis of the unloaded ribs contributed about 3 times increase of the stiffness of the loaded site on average. The rest of the increase in the stiffness, which was estimated three times of increase in average, attributed to the soft constraint imposed on the ribs along the shear directions. For the thorax compression test, the stiffness was higher for the superior area of the thorax for both the mid and the off-centered regions.

During the thorax compression test, the stiffness from the current study was lower than that of the Shaw et al. (2005). There are two possible contributors. First, there have been updates from the THOR-alpha to THOR-Metric dummies. Second, the range of motion of the ball joint from the current study was around 27 degrees, while that from the Shaw et al. (2005) was 12 to 15 degrees depending on the direction of the rotation.

The coupling effects due to the bib were greater for the adjacent levels than that between left and right sides except the rib 1 (See Figure 6). The rib 1 is connected to the opposite side rib via a metal part while other levels of ribs did through rubber-like material. While the sternum exists along the rib 2 to 4, it is just an added mass rather than connecting the two ribs at the same level. The thickness of the bib gets thicker for the rib 5, 6, and 7 compared to the above area. The coupling effect between the adjacent levels was the maximum when the rib 6 was loaded.

The compliance was calculated to understand the contribution of the belt forces applied to the ribs to the IR-TRACC deflection. The compliance information from the rib compression test suggested that the deflections of both the upper and lower thoracic IR-TRACCs mainly resulted from the loading applied to itself and adjacent ribs. For example, the upper thoracic IR-TRACC will be deformed mainly by the forces applied to rib 2, 3, and 4 of the same side. In addition, the IR-TRACC deflection would not be influenced by the forces applied to the opposite side due to the weak coupling between the right and left sides (See Figure 6 and Figure 7). Eggers et al. (2014) performed frontal sled tests using THOR-M50 and investigated the effect of the route of a belt on the IR-TRACC deflection of the thoracic region. The authors tried two belt routes which one of the two was lower than the other by 25.4 mm. In both cases, the belt went through the above of the left-side rib 4, and the lower left thoracic IR-TRACC showed no change in its deflection.

CONCLUSIONS

The current study provided the structural responses of the thorax of the THOR-M50 (Metric) dummy. The provided results can be used for the THOR dummy model validation as well as to understand interactions between the thorax of the THOR dummy and the restraint systems during crash test results.

ACKNOWLEDGEMENT

The authors thank Greg Shaw from University of Virginia Center for Applied Biomechanics for his guidance in reproducing the test condition.

REFERENCES

Cavanaugh, J., Jespen, K., & King, A. (1988). Quasi–static frontal loading on the thorax of cadavers and Hybrid III dummy. In Proceedings on the 16th International Workshop on Human Subject for Biomechanical Research, Atlanta (pp. 3-18).

Eggers, A., Eickhoff, B., Dobberstein, J., Zellmer, H., & Adolph, T. (2014). Effects of Variations in Belt Geometry, Double Pretensioning and Adaptive Load Limiting on Advanced Chest Measurements of THOR and Hybrid III. In Proceedings of IRCOBI Conference.

Lebarbé, M., & Petit, P. (2012, September). New biofidelity targets for the thorax of a 50th percentile adult male in frontal impact. In Proceedings of the 2012 IRCOBI Conference.

Lemmen, P., Hynd, D., Carroll, J., Davidsson, J., Been, B., Song, E., & Steeger, B. (2012). Thoracic injury assessment for improved vehicle safety. Procedia-Social and Behavioral Sciences, 48, 1649-1661.

Shaw, G., Crandall, J., & Butcher, J. (2000, September). Biofidelity evaluation of the THOR advanced frontal crash test dummy. In IRCOBI Conference on the Biomechanics of Impact.

Shaw, G., Lessley, D., Bolton, J., & Crandall, J. (2004). Assessment of the THOR and Hybrid III crash dummies: Steering wheel rim impacts to the upper abdomen (No. 2004-01-0310). SAE Technical Paper.

Shaw, G., Lessley, D., Kent, R., & Crandall, J. (2005, June). Dummy Torso Response to Anterior Quasistatic Loading. In 19th ESV Conference, Paper (No. 05-0371).

Sunnevång, C., Hynd, D., Carroll, J., & Dahlgren, M. (2014, September). Comparison of the THORAX Demonstrator and HIII sensitivity to crash severity and occupant restraint variation. In Proceedings of the IRCOBI Conference, Berlin, Germany.

Yaguchi, M., Ono, K., & Masuda, M. (2008). Biofidelic responses of the THOR-NT and Hybrid III based on component tests (No. 2008-01-0520). SAE Technical Paper.